CONVECTED COORDINATES FOR TRANSIENT NONLINEAR FINITE-ELEMENT ANALYSIS

T. BELYTSCHKO, B.J. HSIEH
College of Engineering, University of Illinois at Chicago Circle, Chicago, Illinois 60680, U.S.A.

J.M. KENNEDY
Engineering Mechanics Section, Reactor Analysis and Safety Division, Argonne National Laboratory, Argonne, Illinois 60439, U.S.A.

SUMMARY

In the transient dynamic finite-element analysis of structures and continua, a key prerequisite for large-scale analyses is an efficient computational scheme. Many of the nonlinear dynamic programs currently available, such as, for example, those of J.A. Stricklin *et al.*, and J.F. McNamara and P.V. Marcal, employ Lagrangian descriptions. Hence, the treatment of geometric nonlinearities requires the use of nonlinear stress-strain relations. In flexural elements, where numerical integration is needed for the computation of nodal forces, these nonlinear terms require considerable computational effort. Hence, these programs are relatively time consuming and the size of problems that can be analyzed is quite restricted.

This paper describes a transient finite-element procedure which uses convected coordinates that rotate with the elements. These convected-coordinate procedures were first described for static analysis in the pioneering works of J.H. Argyris *et al.* However, particularly in the U.S., their usage has been quite limited. Yet the convected-coordinate formulation is especially suited to transient problems, for it simplifies the finite-element relations and consequently results in considerable efficiency.

The method presented here is a variation on the method first presented by Argyris. For problems with small strains but arbitrarily large rotations, it is shown that the relations between strains in the convected coordinates and what are termed deformation displacements are completely linear. Similarly, the relations between nodal forces and element stresses are linear. The nonlinearities that arise from large rotations are treated entirely by the transformations between the elements' convected coordinates and the global coordinates.

The method has been applied to beams and continua in two dimensions, axisymmetric shells and continua, and plates in three-dimensional space. Sample results for all of these problems will be presented and compared with available numerical and experimental results. A major feature of this method is its computational efficiency. On an IBM 370/195, the speed ranges from 1500 to 3000 element steps per second, depending on the element.

— Stricklin, J.A., Haisler, W.E., and Von Riesemann, W.A., "Computation and Solution Procedure for Nonlinear Analysis by Combined Finite Element-Finite Difference Methods, "Natl. Symp. on Computerized Structural Analysis and Design, George Washington University, March, 1972.
— McNamara, J.F. and Marcal, P.V., "Incremental Stiffness Method for Finite Element Analysis of the Nonlinear Dynamic Problem," Pro. Int. Symp. on Numerical and Computer Methods in Struct. Mech., Urbana, Ill., Sept., 1971.
— Argyris, J.H., Kelsey, S., and Kamel, H., "Matrix Methods of Structural Analysis: A Precis of Recent Developments," in B.F. de Veubeke (ed.), Matrix Methods of Structural Analysis, AGARDograph 72, Pergamon Press, (1964).

1. Introduction and Review of Literature

The development of finite element programs for nonlinear, large displacement problems has recently generated considerable interest. The potential of these methods is quite evident, for they can easily handle irregular geometries, inhomogeneities and interfaces between continua and structures. However, many finite element programs for transient nonlinear analysis, when compared to finite difference methods, are quite inefficient. Thus, the versatility of finite element programs is achieved with a significant loss of economy and the solution of large scale models is often prohibitively expensive. This paper reviews the computational merits and disadvantages of various schemes that have been used in nonlinear, transient finite element techniques and describes a "convected" element procedure that has been found to be particularly effective for many problems of reactor safety analysis.

The finite element equations for problems nonlinear in both geometry and material were first formulated by Oden [1,2], who employed a Lagrangian description. Lagrangian descriptions were subsequently also used by Wu and Witmer [3], who solved a series of problems using beam elements, by Stricklin, Haisler, and Von Riesemann [4,5], who solved an extensive series of axisymmetric shell problems, and by McNamara and Marcal [6]. Recently, mixed Lagrangian-Eulerian formulations have been used by Hartzman and Hutchinson [7] and Heifitz and Costantino [8]. The former formulated the equations of motion in terms of Eulerian (Cauchy) stresses, but expressed the constitutive equations in terms of Lagrangian (Kirchhoff) stresses and increments in Lagrangian strain. The latter used Eulerian strains and stresses with a Jaumann rate but updated the coordinates at every time step. Hence, the latter scheme is basically Eulerian; the only difference between it and a complete Eulerian description is the use of a mesh that moves with the material.

These previous finite element procedures for nonlinear problems can be classified from two aspects: the type of kinematic, kinetic and mesh description (Lagrangian, Eulerian or mixed) and the type of temporal integration (implicit, explicit). Each of these techniques has its particular merits and shortcomings and often the ideal combination depends on the nature of the problem to be solved.

Most of the previous work for nonlinear transient analysis has been in terms of a Lagrangian description [Refs. 1 to 6]. Lagrangian descriptions have several important advantages: (1) the constitutive equations are independent of the material rotation and (2) boundaries and inhomogeneities are easily treated. One disadvantage is that for very large strains the finite element mesh is excessively distorted. A more serious shortcoming in engineering applications is that both the strain-displacement and nodal force-stress relations include quadratic combinations of the shape functions. The evaluation of these terms is computationally very demanding, especially in elements that require numerical quadrature.

Eulerian and quasi-Eulerian procedures such as [6] and [7] are computationally more efficient because the incremental strain-displacement and nodal force-stress relations involve only linear terms. This benefit, however, is obtained at the cost of several significant disadvantages: (1) the stress-strain relationships for anisotropic materials in Eulerian descriptions vary as the material rotates and (2) the treatment of boundaries and inhomogeneities is complicated. Hartzmann and Hutchinson circumvented the first difficulty by expressing the constitutive equation in Lagrangian variables and then transforming to Eulerian stress before applying the equations of motion. Heifitz and Costantino used Eulerian variables throughout and they did not transform their stress-strain equations as the material

rotates. Therefore, their formulation is restricted to isotropic materials and is not applicable to fiber reinforced materials or elastic-plastic materials that harden kinematically.

The difficulties inherent in Eulerian treatments of boundaries and inhomogeneities are well known. Heifitz and Costantino avoided these difficulties by updating the geometry at each time step, which is essentially then a Lagrangian mesh. This procedure insures that boundaries and interfaces between different materials continue to coincide with element sides, rather than moving through elements. However, updated configurations are effective only for elements with displacement fields that vary linearly along the sides. For higher order elements, such as those used in beams and plates, the updated configuration becomes curvilinear and the computations in terms of Eulerian quantities become very involved. Thus, the advantages of Eulerian and quasi-Eulerian schemes seem to be limited to isotropic materials and linear displacement type elements.

The second alternative in a transient finite element formulation is the temporal integration. Implicit integration was used in Refs. 2,4,5 and 6, while explicit integration was used in Refs. 3,7 and 8. As is well known, implicit integration schemes can be stable, regardless of the size of the time step, whereas explicit integration schemes are unstable unless the time step is sufficiently small. Implicit integration schemes, however, require matrix inversions, while explicit schemes generally do not require inversions. The choice of integration procedure is also intimately related to the choice of mass matrix; the use of consistent mass matrices with explicit integration is self-defeating, for then a matrix inversion is still needed. On the other hand, the additional expense due to the use of a consistent mass is minute in implicit schemes.

Krieg and Key [9] have provided some most interesting insights into the comparative advantages of these methods by showing that the spectral errors due to lumped mass discretization and explicit temporal integration are opposite in sense; i.e., that they tend to cancel, and that similarly the spectral errors of consistent mass discretization and implicit integration are opposite. On the other hand, they showed that the errors in lumped-implicit and consistent-explicit schemes are cumulative. Hence, lumped-explicit and consistent-implicit schemes are ideal combinations from both aspects of accuracy and efficiency.

The choice among these two methods then depends mostly on the nature of the loading, material and finite element mesh. For rapid loadings, the stability limitations on the time step are not critical, since an accurate determination of the response requires a small time step anyway. A small time step is also required for highly path-dependent materials, such as elastic-plastic materials, for unloading always takes place in transient problems, so the use of linearizations over large time steps in implicit integrations may lead to sizable errors.

The comparative computational merits depend mostly on the scale of the problem. Since in nonlinear, large displacement problems the stiffness and consistent mass matrices vary with time, they must both be recomputed, combined and inverted at every time step. The inversion takes NB^2 computations, where N is the number of degrees of freedom and B the semi-bandwidth, and the computation of the stiffness and mass matrices is also time consuming. In explicit-lumped schemes, the number of computations is directly proportional to the number of nodes. Therefore, it is apparent that for very large systems, explicit-lumped schemes will be far more economical; implicit-consistent schemes are most suitable for small bandwidth meshes with very high frequencies, such as isolated shells.

2. Convected Element Procedure

The nonlinear finite element programs developed by the authors use a convected coordinate procedure which was first applied to transient problems by Belytschko and Hsieh [10,11]. The term convected coordinates here designates a coordinate system that rotates and translates with the element; they are distinguished from Lagrangian coordinates in that they do not deform with the element. Since the term convected coordinates is often applied to Lagrangian (material) coordinates, this term may be confusing and more appropriate nomenclature may be "translated-rotated," or "rigid-convected" coordinates. However, for the sake of simplicity, we will continue to use the term "convected" coordinates and caution the reader of these ambiguities.

The formulation discussed here is suitable for problems with large rotations and small deformations, problems where the engineering strains, such as those recorded by a strain gauge, are small. In that case, the strains in the convected coordinates are linearly related to what are termed "deformation" displacements, which are the displacements relative to the convected coordinates. Moreover, within the convected coordinates, the nodal forces are related to the stresses by relationships that are linear in the shape functions. These linearities streamline the computational procedure, particularly in flexural elements which require numerical quadrature through the thickness.

Convected coordinate procedures have previously been applied to static analysis by Argyris, Kelsey and Kamel [12], Wempner [13] and Murray and Wilson [14]. But the methods are particularly suited to nonlinear transient problems, because the computational simplifications in the nodal force-stress and strain-displacement computations are crucial in dynamic analysis, whereas in static analysis matrix inversion accounts for the bulk of the computations. Yet, much previous work in transient analysis has failed to take advantage of these simplifications.

To begin, let $\hat{x}_I$ denote a coordinate system which translates and rotates with element I. The displacement field for each element is subdivided into a pure deformation, u_i^{def}, and a pure rigid body motion u_i^{rig}, so that

$$u_i = u_i^{def} + u_i^{rig} \tag{1}$$

The deformation is assumed to precede the rigid body motion. According to the polar decomposition theorem of continuum mechanics, the angle of rigid body rotation can be found for any displacement field, so the above decomposition can always be accomplished.

If we view the deformation of the element in terms of coordinate transformations, then the pure deformation can be described by

$$\hat{x}_i = (\delta_{ij} + \alpha_{ij})X_j \quad \text{(repeated indices not enclosed by parenthesis denote summations)} \tag{2}$$

where $\hat{x}_i$ and X_j are the convected and Lagrangian (material) coordinates, respectively, α_{ij} is a symmetric transformation, and δ_{ij} is the Kronecker delta. The succeeding rigid body motion then completes the transformation as follows

$$x_i = t_i + a_{ij}(\delta_{jr} + \alpha_{jr})X_r \tag{3}$$

where x_i are the Eulerian (spatial) coordinates, a_{ij} is an orthogonal transformation and t_i represents the rigid body translation. The displacement field is then given by

$$u_i = x_i - X_i = t_i + a_{ij}\alpha_{jr}X_r \tag{4}$$

whereas the deformation displacements in the global and convected coordinates are given by

$$u_i^{def} = a_{ir}\alpha_{rj}X_j$$
$$\hat{u}_i^{def} = \alpha_{rj}X_j \tag{5}$$

In a finite element procedure, the displacement field in each element is represented by shape function $\phi_{jn}(\hat{x})$, so that

$$u_i = \phi_{iN}(\hat{x})d_N^{(I)} \tag{6}$$

where d_N are the nodal variables of element I. If the shape functions are complete, they must be capable of representing rigid body motion. Thus, the deformation displacements can also be expressed in terms of ϕ_{iN}

$$\hat{u}_i^{def} = \phi_{iN}(\hat{x})d_N^{(I)def} \tag{7}$$

Moreover, since the rigid body modes are absent from $d_N^{(I)def}$, the order of this matrix is less than that of $d_N^{(I)}$ by the number of rigid body modes.

The strains in the convected coordinates are defined by

$$\hat{\varepsilon}_{ij} = \frac{1}{2}\left(\hat{u}_{i,j}^{def} + \hat{u}_{j,i}^{def}\right) \tag{8}$$

where commas denote differentiation with respect to the convected coordinates.
From eqs. (5) and (8), it can be shown that

$$\hat{\varepsilon}_{ij} = \alpha_{ij} + O^2(\alpha_{ij}) \tag{9}$$

Hence, if α_{ij} are small, then $\hat{\varepsilon}_{ij}$ is a measure of the distortion and can be viewed as an engineering measure of strain. Furthermore, if α_{ij} are small, the convected strains are equal to the Green (Lagrangian) strains.

From eqs. (7) and (8), it follows that

$$\hat{\varepsilon}_{ij} = \frac{1}{2}\left(\phi_{iN,j} + \phi_{jN,i}\right)\hat{d}_N^{def} \tag{10}$$

The variation of internal work is given by

$$\delta W^{int} = \int_{V_I} \delta\hat{\varepsilon}_{ij}\hat{\sigma}_{ij} \tag{11}$$

where $\hat{\sigma}_{ij}$, the convected stresses, correspond to Cauchy (Eulerian) stress components in the rotated coordinates if α_{ij} are small. If we apply the principle of virtual work and include inertial forces in a d'Alembert sense, we find that

$$\sum_I \int_{V_I} \delta\hat{\varepsilon}_{ij}\sigma_{ij} - \delta d_N F_N^{ext} - \delta d_M M_{MN}\ddot{d}_M = 0 \tag{12}$$

where F_N^{ext} are the external forces, M_{NN} is the mass matrix, and superscript dots denote time derivatives. The first term in eq. (12) can be expanded by using eq. (10)

$$\int_{V_I} \delta\hat{\varepsilon}_{ij}\hat{\sigma}_{ij} = \delta d_N^{(I)def} \int_{V_I} \phi_{iN,j}\hat{\sigma}_{ij} \tag{13}$$

and making use of the fact that element nodal forces are self-equilibrated, it follows

that

$$\delta d_N^{(I)rig} \int_{V_I} \phi_{iN,j} \hat{\sigma}_{ij} = 0 \tag{14}$$

By adding eqs. (12) and (14) and utilizing the arbitrariness of the variations, it follows that

$$\sum_I L_{NM}^{(I)} \int_{V_I} \phi_{iM,j} \hat{\sigma}_{ij} - F_N^{ext} - M_{NM} \ddot{d}_M = 0 \tag{15}$$

where $L_{NM}^{(I)}$ is the connectivity matrix described in Ref. [2]. This equation can be put into very simple matrix form; let $\phi_{iM,j}$ be arranged in a matrix [E] with the permutations of indices i and j corresponding to the rows of [E] and the index M corresponding to column numbers and let σ_{ij} be similarly placed in a column matrix $\{\hat{\sigma}\}$. Then

$$\sum_I [L]^T \int_{V_I} [E]^T \{\hat{\sigma}\} - \{F^{ext}\} - [M]\{\ddot{d}\} = 0 \tag{16}$$

The principal feature of this equation is the simplicity of the integral expression for internal nodal forces; ϕ appears only linearly and the expression is thus amenable to matrix form. In the Lagrangian formulation, ϕ appears quadratically and a matrix form cannot be obtained. Furthermore, the expression reflects the total nodal forces. Other convected coordinate formulations, such as that of Argyris, et al, are incremental. The use of total relations may be advantageous in transient analyses for they eliminate a source of truncation error.

This convected coordinate formulation has been used in three computer programs: WHAM (Waves in Hysteretic Arbitrary Media), STRAW (Structural Transient Response of Assembly Wrappers), and SADCAT (Structural Analysis for Three-Dimensional Core Assembly Transients). WHAM is applicable to two-dimensional and three-dimensional axisymmetric problems and it includes both continuum and flexural elements. The treatment of axisymmetric problems by convected coordinates is described in Ref. [11]. STRAW is a special purpose version of WHAM which includes features such as quasi-Eulerian description over portions of the mesh and sliding interfaces. SADCAT is a three-dimensional code which is under development.

All of the programs use an explicit integration and a lumped mass matrix. In continuum elements, the lumped masses are obtained by equally apportioning the mass of each element among its nodes. When an element has rotational degrees of freedom, its mass moment is also equally apportioned among its nodes. In three-dimensional problems, the principal coordinates of the mass moment tensor are then found at each node and the rotational equations of motion are expressed in these rotating, principal coordinates.

The computational procedure used in these programs is shown in Fig. 1. Because of the use of an explicit-lumped scheme, the programs are architecturally very simple. A rudimentary version of the WHAM code for two-dimensional problems requires less than 400 FORTRAN statements; the latest version of WHAM with both axisymmetric and plane capabilities and extensive input-output features involves 1600 FORTRAN statements. Storage requirements are also low; in WHAM the words of storage needed is approximately

$$w = 11n_{ec} + 30n_{eb} + 12n_n$$

where n_n is the number of nodes, n_{eb} and n_{ec} the number of continuum and flexural elements; the bulk of the storage is used to record the stress and strain histories.

3. Examples

In this section, three sample problems that have been solved by STRAW and WHAM are presented:

(1) a clamped ring loaded impulsively;

(2) a circular plate loaded impulsively;

(3) a one-twelfth section of a loaded hexagonal reactor fuel subassembly and the adjacent subassemblies.

Experimental results for the first problem were obtained by Balmer and Witmer [15] and finite element results have previously been given by Wu and Witmer [3]. The results presented here for the first problem have been previously presented in greater detail by Belytschko and Hsieh [10].

The clamped ring was manufactured from aluminum and its yield stress and Young's modulus were 42,800 psi and 10.5 x 10^6 psi, respectively. An impulsive loading of 4862 in/sec was applied as shown in Fig. 2. The cross-section of the beam was 1/8 in. thick and 1.2 in. wide, so most of the structure is in a state of plane strain.

The problem was solved by STRAW with 16 rectilinear beam elements for the half ring. Because beam elements treat the state of stress as uniaxial, an exact treatment of plane strain in the plastic range is not possible, for while in the elastic range the transverse stress σ_t is given by $\nu\sigma_\ell$ (ν is Poisson's ratio), in the plastic domain the ratio of σ_t to σ_ℓ varies with time. Therefore, plane strain cannot be treated exactly without storing the transverse stresses, which is quite undesirable. In this program, the plane strain problem is treated in an approximate manner, as follows. Since prior to initial yielding, $\sigma_t = \nu\sigma_\ell$, it is apparent that the von Mises yield criterion gives

$$\sigma_\ell^2 - \nu\sigma_\ell^2 + \nu^2\sigma_\ell^2 \leq \sigma_o^2 \tag{17}$$

so that the condition for elastic response is

$$\sigma_\ell^2 \leq \frac{\sigma_o^2}{1-\nu+\nu^2} \tag{18}$$

In the usual fashion for elastic plane strain analysis, E_e' was given by

$$E_e' = \frac{E_e}{1-\nu^2} \tag{19}$$

while E_p' was assumed to be given by

$$E_p' = \frac{3}{2} E_p \tag{20}$$

This formula is based on the assumption that subsequent to yielding, the ratio of transverse to longitudinal stresses shifts to approximately 1/2 as required by the Mises flow law.

Another corrective factor employed in obtaining these results is the modification of the cross-sectional area to account for the incompressibility of the plastic strains. This is accomplished by computing the area by the formula

$$A = A_o(1-\epsilon_m) \tag{21}$$

where A_o is the original area and ϵ_m the midplane strain. This formula neglects the effects of flexural strains on the change of cross-sectional area of each sublayer of the beam. However, in the Euler-Bernoulli beam theory, the net change in cross-sectional area due to

flexural strains vanishes, so eq.(21)is probably adequate in reflecting the net effects of incompressibility.

Results for displacements are given in Fig. 3, along with finite difference and finite element results obtained in Ref. [3]. It can be seen that the results obtained here match the experimental results quite well. The finite element and difference results given in Ref. [3] fall substantially below and above the experimental results, respectively. In the results of Ref. [3] the effects of plane strain and incompressibility were evidently not included. In this problem, the midplane strains at 1800μsec are all compressive, with a maximum of 4%, so the effect of incompressibility is to increase the cross-sectional area, strengthen the ring, and reduce the response. Similarly, the plane strain effects reduce the response. Hence, the overshoot in the finite difference response can be explained. The undershoot in Wu and Witmer's finite element results cannot be explained by these factors. However, the finite element results were obtained by an explicit-consistent scheme. According to Krieg and Key (9), this is a particularly poor combination and may cause the observed discrepancies.

The second example is a circular plate clamped as shown in Fig. 4. Experimental and finite difference results obtained by DEPROSS have been given for this problem by Duffey and Key [16], and are given along with the finite element results, WHAM, in Figs. 5 and 6. The stress-strain curve here was based on the data given in Ref. [16]: $E_e = 28.4(10^6)$ psi, $E_p = 4.6(10^5)$ psi, $\sigma_o = 8.1(10^4)$ psi. Beyond $9.0(10^4)$ psi, the material was assumed to behave in a perfectly plastic manner; isotropic strain hardening was used.

In the finite element results obtained here, the plate was clamped at 5 in. and supported by rollers over the outer 2 inches; in Ref. [16] the plate was clamped at 3 in. Equal elements 1/4 in. long were used in the finite element mesh, while Ref. [16] used a 1/8 in. grid spacing.

As can be seen, both sets of results match the experimental results quite well, though the finite difference results match the early peak strains and displacements more closely, while the finite element results match the later response and period better. The improved behavior at peaks in the finite difference results is to some extent the result of the finer mesh, but a more significant cause is the boundary conditions.

The plates were fixed by torqueing the twelve bolts at the clamp to 85 ft-lb. Hence, initially the plates were nearly perfectly constrained from horizontal motion at the clamps. As the membrane stress wave travels through the plate, axial displacement of the order 0.1 inches result. This corresponds to an average radial strain of about 5% and an average hoop strain of about -3% in the clamped region. Because of incompressibility, the thickness strain is then -2%. In view of this extremely large compressive thickness strain, it is evident that the clamping constraint cannot be maintained longitudinally once the maximum membrane response is achieved, which explains why the DEPROSS results, based on a clamp at 3 in., are better at early times, while the WHAM results, based on a roller from 3 in. to 5 in., are better at larger times.

The third problem presented here is a 1/12th plane section (Fig. 7) of a loaded hexagonal subassembly and the adjacent hexagonal can for a LMFBR. In this model, both the coolant layer between the hexcans and the innards of the adjacent hexcan have been modelled. The elements corresponding to the sodium layer between two layers are quasi-Eulerian elements which do not move with the material; their positions are determined by the positions of the

beams. The tangential velocities in the sodium interface are independent of the tangential velocities of the hexcan walls and a viscous force is introduced which depends on the relative magnitudes of their tangential velocities. In addition, the program can account for the transverse motion of the sodium, though this feature was not used in obtaining these results.

The hexcan walls are stainless steel with an elastic modulus of $23.49(10^6)$ psi, a yield stress of $5.7(10^4)$ psi; beyond the yield stress isotropic hardening with a hardening parameter of $3.45(10^6)$ psi was used. All material properties were modified as given in eqs. 18 to 20 to account for a state of plane strain.

Figs. 8 and 9 report the displacements at the midpoint of the loaded hexcan flat and the inside strains at the corner, respectively. Results are also given for an isolated hexcan subjected to an identical loading.

The 409 element mesh shown here required 125 sec of computer time for a solution of 1500 time steps. This corresponds to 5000 mesh elements per second; i.e., a 5000 element mesh requires one second per time step.

4. Conclusions

Because of the iterative nature of transient solutions, the achievement of economy in the computational procedure is quite important. The convected coordinate procedure described in this paper simplifies the equations which are used in explicit integration procedures, and as evidenced by the running times, yields a very efficient computer program that makes possible the analysis of relatively large problems. Because closed form solutions are not available for this type of problem, definitive assessments of the comparative accuracy of these computational procedures are not possible. Comparison with experiments shows that the results are sufficiently accurate for most engineering purposes and that in many cases, the discrepancies are as much a consequence of shortcomings of the experimental apparatus as of the computer programs.

References

[1] ODEN, J. T., "Finite Element Applications in Linear and Nonlinear Thermoviscoelasticity," EMD Specialty Conference, ASCE, (1967).

[2] ODEN, J. T., Finite Elements of Nonlinear Continua, McGraw-Hill Publishing Co., New York, (1972).

[3] WU, E. H., and WITMER, E. A., "Finite Element Analysis of Large Elastic-Plastic Transient Deformations of Simple Structures," AIAA Journal, Vol. 9, pp. 1719-1724, (1971).

[4] STRICKLIN, J. A., HAISLER, W. E. and VON RIESEMANN, W. A., "Computation and Solution Procedure for Nonlinear Analysis by Combined Finite Element-Finite Difference Methods," Nat'l. Symp. on Computerized Structural Analysis and Design, George Washington University (1972).

[5] STRICKLIN, J. A. and HAISLER, W. E., "Evaluation of Solution Procedures for Material and/or Geometrically Nonlinear Structural Analysis," AIAA Journal, Vol. 11, pp. 292-299 (1973).

[6] MCNAMARA, J. F. and MARCAL, P. V., "Incremental Stiffness Method for Finite Element Analysis of the Nonlinear Dynamic Problem," Pro. Int. Symp. on Numerical and Computer Methods in Structural Mechanics, Urbana, Illinois (Sept., 1971).

[7] HARTZMAN, M. and HUTCHINSON, J. R., "Nonlinear Dynamics of Solids by the Finite Element Methods," Computers and Structures, Vol. 2, pp. 47-77 (1972).

[8] HEIFITZ, J. H. and COSTANTINO, C. J., "Dynamic Response of Nonlinear Media at Large Strains," J. of Eng. Mech. Div., ASCE, pp. 1511 (1972).

[9] KRIEG, R. D. and KEY, S. W., "Transient Shell Response by Numerical Time Integration," 2nd U. S. Japan Seminar on Matrix Methods in Structural Analysis, Berkeley, California (1972).

[10] BELYTSCHKO, T. and HSIEH, B. J., "Nonlinear Transient Finite Element Analysis with Convected Coordinates," to be published Intl. J. of Num. Methods in Eng. (1972).

[11] BELYTSCHKO, T., and HSIEH, B.J.,"Nonlinear Transient Analysis of Shells and Solids of Revolution by Convected Elements," AIAA/ASME/SAE 14th Structures, Structural Dynamics, and Materials Conf., Williamsburg, Va., Mar. 20-22, 1973.

[12] ARGYRIS, J. H., KELSEY, S. and KAMEL, H., "Matrix Methods of Structural Analysis: A Precis of Recent Developments," Matrix Methods of Structural Analysis, B. F. deVeubeke (ed.), AGARDograph 72, Pergamon Press (1964).

[13] WEMPNER, G. A., "Finite Elements, Finite Rotations and Small Strains of Flexible Shells," Intl. J. Solids Struct., Vol. 5, pp. 117-153 (1969).

[14] MURRAY, D. W. and WILSON, E. L., "Finite Element Large Deflection Analysis of Plates," J. Eng. Mech. Div., ASCE, Vol. 95, pp. 145-163 (1969).

[15] BALMER, H. A. and WITMER, E. A., "Theoretical-Experimental Correlation of Large Dynamic and Permanent Deformations of Impulsively Loaded Simple Structures," FDL-TDR-64-108, Air Force Flight Dyn. Lab., Wright-Patterson AFB, Ohio.

[16] DUFFEY, T. A. and KEY, S. W., "Experimental-Theoretical Correlations of Impulsively Loaded Clamped Circular Plates," Exp. Mech., (June, 1969).

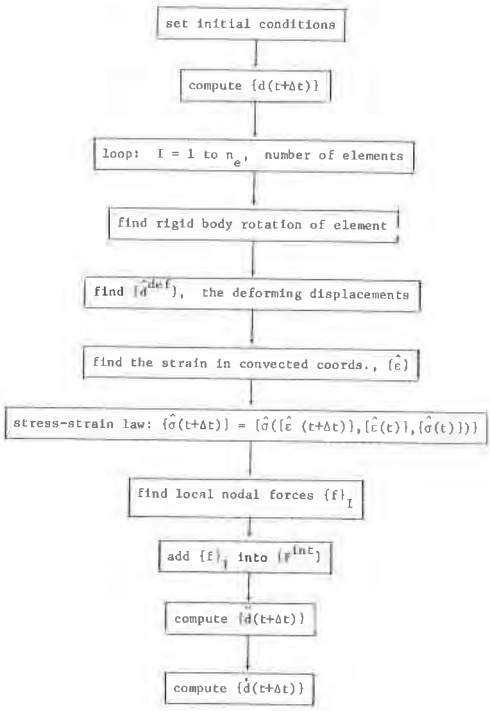

Fig (1) Flowchart of Computational Procedure.

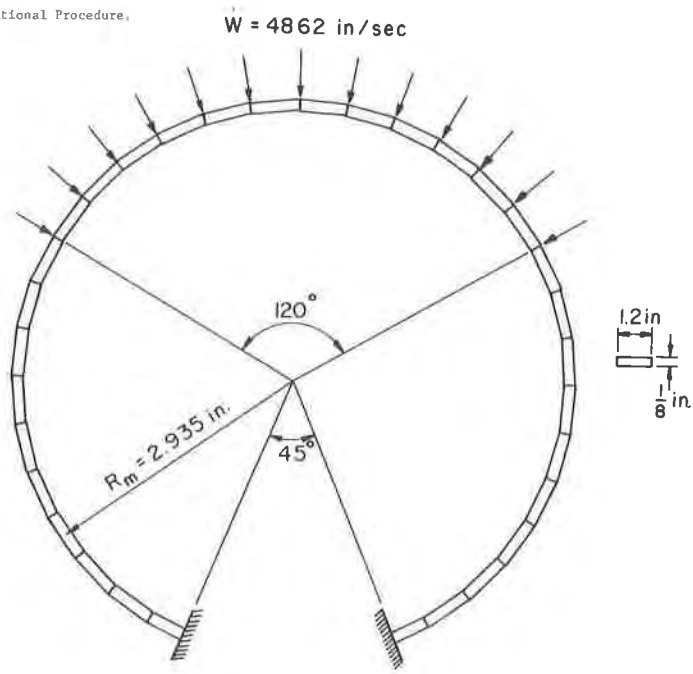

Fig (2) 6061-T6 Aluminum Clamped Circular Ring Geometry and Explosive Loading.

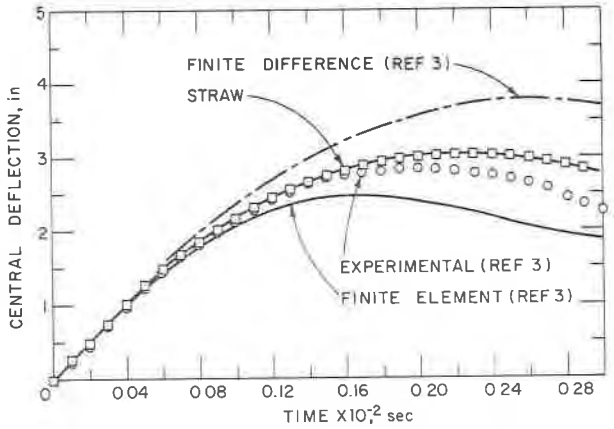

Fig (3) Central Deflection Response for Explosively-Loaded 6061-T6 Aluminum Clamped Circular Ring.

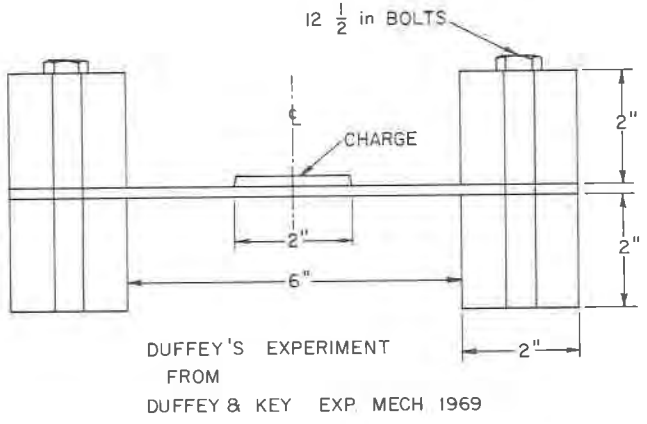

Fig (4) Steel Clamped Circular Plate Geometry and Explosive Loading.

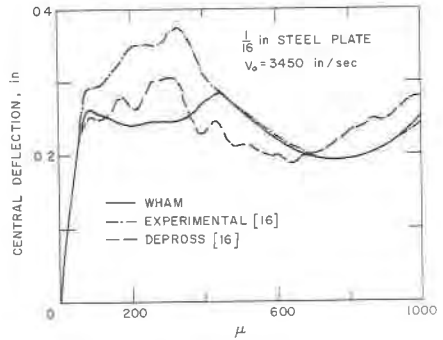

Fig (5) Central Deflection Response for Explosively Loaded Steel Clamped Circular Plate.

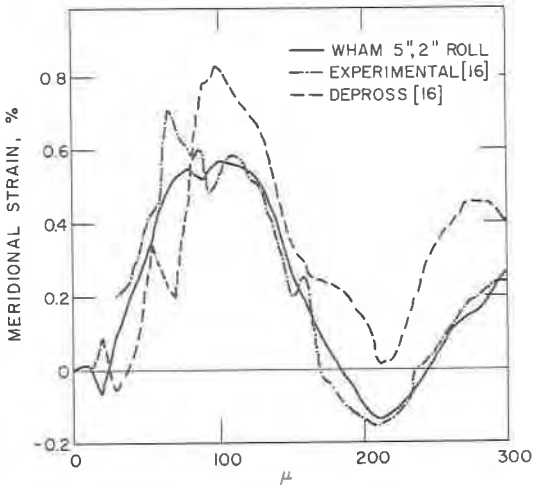

Fig (6) Meridional Strain Response for Explosively Loaded Steel Clamped Circular Plate.

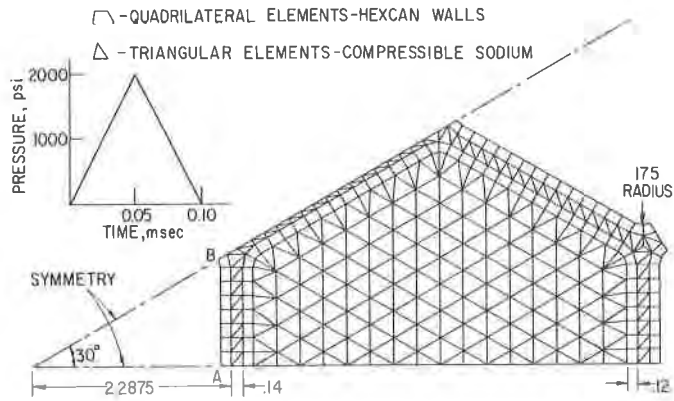

Fig (7) Finite Element Model of LMFBR Core Subassemblies and Pressure-time Loading.

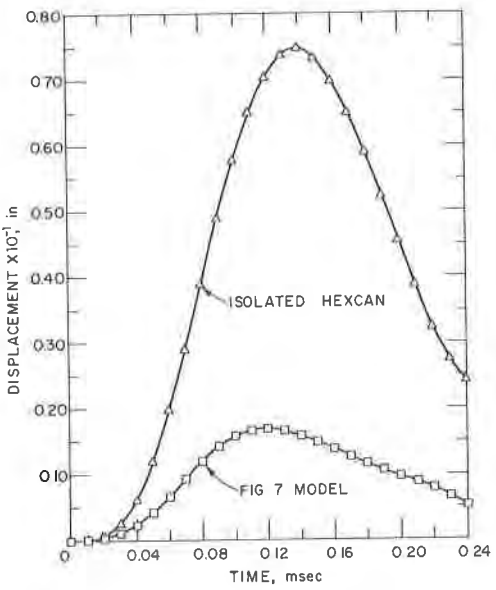

Fig (8) Displacements at Midpoint of Pressure Loaded LMFBR Subassembly Hexcan Flat (Point A).

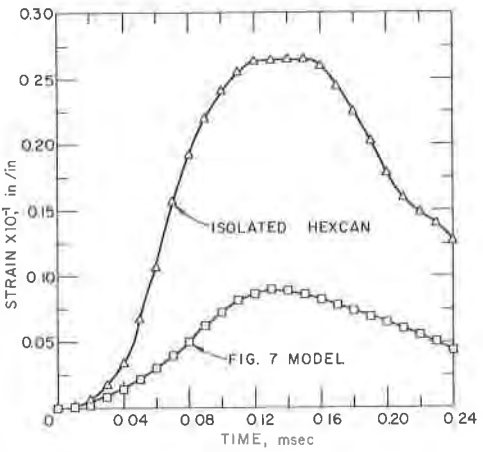

Fig (9) Strains at Inside of Corner of Pressure Loaded LMFBR Subassembly Hexcan Corner (Point B).